Comparison of Three Schemes of Two-Photon Laser-Induced Fluorescence for CO Detection in Flames.

Rosell, Joakim; Sjöholm, Johan; Richter, Mattias; Aldén, Marcus

Published in:
Applied Spectroscopy

DOI:
10.1366/12-06704

2013

Comparison of Three Schemes of Two-Photon Laser-Induced Fluorescence for CO Detection in Flames

Joakim Rosell,* Johan Sjöholm, Mattias Richter, Marcus Aldén

Division of Combustion Physics, Lund University, Box 118, S-22100 Lund, Sweden

Two-photon excitation laser-induced fluorescence of carbon monoxide suffers from interference from mainly C_2 and strong pressure quenching. This paper presents an investigation of three excitation/detection schemes for two-photon excitation laser-induced fluorescence on carbon monoxide. The schemes are evaluated for pressure and quenching partner dependencies and C_2 interference. Three different emission bands lie in the Hopefield-Birge system: The Ångström $B^1\Sigma^+ \rightarrow A^1\Pi_u$ band, with two-photon excitation through $B^1\Sigma^+ \leftarrow X^1\Pi$ around 230 nm; the Herzberg band $C^1\Sigma^+ \rightarrow A^1\Pi_u$, with two-photon excitation through, $C^1\Sigma^+ \leftarrow X^1\Pi$, around 217 nm; and the third positive group $b^3\Sigma \rightarrow a^3\Pi$, also with excitation of $B^1\Sigma^+ \leftarrow X^1\Pi$ around 230 nm. The measurements are performed in laminar premixed flames with various equivalence ratios as well as in a high-pressure cell, where pressure and species concentrations are varied in order to investigate the fluorescence quenching dependence.

Index Headings: **Carbon monoxide; CO; C2; Laser-induced fluorescence; LIF; Ångström; Herzberg; Third positive; Two-photon.**

INTRODUCTION

Detection of carbon monoxide (CO) is of great interest in combustion research. CO emission from combustion devices is regulated all over the world, and a more detailed understanding of CO formation and its release from combustion processes could contribute to a healthier environment. Combustion efficiency is also indicated by CO, since a major part of the heat release in hydrocarbon flames originates from CO oxidation to CO_2;[1] hence the presence of CO is typically an indication of incomplete combustion. In situ detection of CO is therefore of significant interest for various apparatuses. Smyth and Crosley[2] list different diagnostic methods for measurements of CO, emphasizing laser-induced fluorescence (LIF) as the most successful technique for studying CO in combustion environments.

For molecules such as H_2, H_2O, NH_3, and CO that do not have accessible excitation frequencies in the UV/visible region but have resonances in the vacuum ultraviolet (VUV) region, i.e., wavelengths between 100 and 200 nm, two-photon LIF can be used to reach the desired energy level of the molecule.[1,3–6] Many investigations have been done to measure important parameters that affect the different processes that the CO molecule will undergo in two-photon LIF, e.g., absorption and excitation cross section,[7] spectral broadening,[8] collisional quenching,[9,10] photoionization,[11] and fluorescence lift times.[12,13]

For two-photon CO LIF in combustion systems, the most common excitation wavelength is 230.1 nm, matching the $B^1\Sigma^+ \leftarrow X^1\Sigma^+$ transition. The $B^1\Sigma^+ \rightarrow A^1\Pi_u$ Ångström band in the visible region (400–600 nm) is then used for detection.[14–19] Also 217.5 nm excitation of the $C^1\Sigma^+ \leftarrow X^1\Sigma^+$ transitions with subsequent fluorescence through $C^1\Sigma^+ \rightarrow A^1\Pi_u$, i.e., the Herzberg band at 360–600 nm, has been demonstrated.[6] Figure 1 shows a schematic energy diagram for these levels and transitions.

Unfortunately excited C_2 created by photodissociation also emits fluorescence around 430–700 nm, i.e., the Swan bands. This crosstalk with CO LIF measurements is mainly with the Ångström bands of CO (from 230.1 nm excitation) but also to a certain degree with the Herzberg bands (from 217.1 nm excitation). In many combustion environments this reduces the number of useful emission lines for CO detection. This in turn affects the collected signal intensity and, hence, the precision and accuracy as well as the detection limit.[19]

As C_2 can be formed through laser photolysis of CO or of hydrocarbon fuels, due to the short laser wavelength required for CO LIF, the spectral interference from C_2 is very hard to eliminate.[15,20] To avoid C_2 crosstalk, the LIF signal from the $b^3\Sigma^+ \rightarrow a^3\Pi$ third positive bands of CO around 282–380 nm could potentially be used. The $b^3\Sigma$ triplet state is energetically close to the $B^1\Sigma^+$ singlet state and can be populated through collisions.[15] The aim of this study is to investigate and compare the signals originating from the three CO LIF bands stated earlier (see Fig. 1) regarding C_2 crosstalk, pressure, and quenching partner dependences. This is done in a cell, where pressure and quenching species are varied, and in laminar premixed flames.

EXPERIMENTAL SETUP

The experimental setup for the measurements is illustrated in Fig. 2. The laser used in this setup was a Nd:YAG laser system from Thales Laser (repetition rate 10 Hz). The laser radiation was frequency tripled to 355 nm, and pulse energies of 300 mJ were used to pump an Optical Parametric Oscillator (OPO). The OPO system consists of a midband OPO PremiScan/MB (GWU Lasertechnik Vertriebsges, mbH, Germany) and a wave meter.[21,22]

Working with an OPO system has many benefits compared to working with dye lasers, e.g., compactness and ease of alignment and operation. Depending on which band in the Hopfield-Birge system that was excited, the OPO output was tuned to either 460.13 or 435.11 nm, both with a spectral width of ~4 cm^{-1}. The spectral widths of the excited CO absorption bands are all broader than the spectral width of the laser; i.e., sufficient spectral overlap and corresponding high excitation efficiency is expected. After the OPO a BBO crystal was used for frequency doubling. To separate the UV beam from the fundamental beam a Pellin-Broca quartz prism was used. The UV beam was focused using two quartz lenses; a spherical $f =$

Received 26 April 2012; accepted 30 October 2012.
* Author to whom correspondence should be sent. E-mail: joakim.rosell@forbrf.lth.se.
DOI: 10.1366/12-06704

0003-7028/13/6703-000000/0

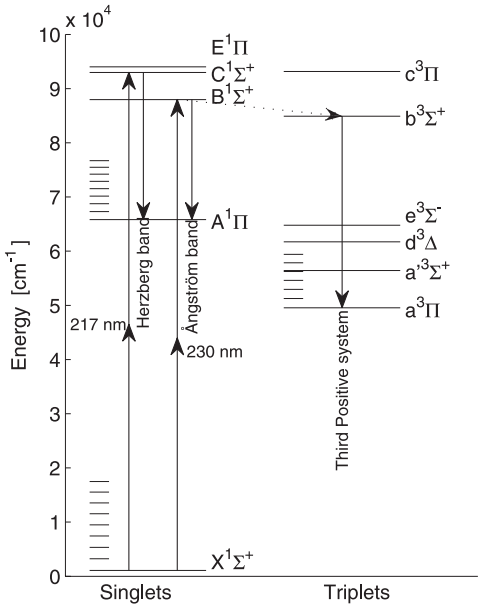

FIG. 1. A schematic energy-level diagram for the electronic levels and transitions cited in this paper. Shorter lines indicate vibrational levels.

300 mm and a cylindrical $f = 200$ mm lens. Due to some variations in OPO and doubling crystal (BBO) conversion efficiency the laser pulse energy of the 217 nm at 1.3 mJ beam was always $\sim$50% less than the pulse energy of the 230 nm beam at 2.7 mJ, resulting in a lower LIF signal for the 217 nm case. The laser pulse duration was 10 ns.

The fluorescence light was collected with an UV-achromatic Bernhard Halle $f = 100$ mm, $f_{\#} = 2$ lens, which imaged the light onto the entrance slit of an Acton 2300i spectrometer. The spectrometer had a grating of 300 grooves/mm at a blazing angel optimized for 300 nm (Fig. 3 shows the grating efficiency curve). The optimum slit width was determined to be 300 μm using a reference spectral (Hg) lamp and investigating the peak intensities and full with at half maximum (FWHM) as a function of the slit width. A slit width of 300 μm led to a measured FWHM of 1 nm for the 460 nm and 435 nm laser light lines on the detector.

Detection was made with a Princeton PI-MAXII Intensified CCD camera that was mounted on the spectrometer. For increased signal-to-noise ratio hardware binning of 2×2 pixels was used, leading to a resolution of 521×512 pixels and a dispersion of 0.27 nm/pixel. The gate width of the camera was set to 100 ns for the cell measurements and 30 ns for the flame measurements in order to further suppress background light.

Efficiency curves for the camera and spectrometer are shown in Fig. 3. Multiplying them with each other and normalizing to unity gives the normalized total efficiency curve also seen in Fig. 3.

To suppress elastically scattered laser light, a N,N-dimethylformamide liquid filter with an optical absorption length of 12 mm is placed in front of the slit of the spectrometer. Figure 4 shows the filter transmission between 230 and 560 nm. This filter is an effective long-pass filter that blocks wavelengths below 270 nm.

For the cell measurements a high-pressure cell with three quartz window (50 mm in diameter) was used. This allowed the laser light to pass through and the signal to be collected at a right angle to the laser beam. A pressure meter was also coupled to the cell.

The cell was prior to the measurements evacuated using a vacuum pump. Then 0.1 bar CO was injected into the cell, and for subsequent measurements the partial pressure of the colliding partner gas was gradually increased until the total pressure reached 5 bar. The gases of interest were N_2, air, and propane (C_3H_8).

For the flame measurements the cell was replaced by a water-cooled laminar tube burner with an opening diameter of

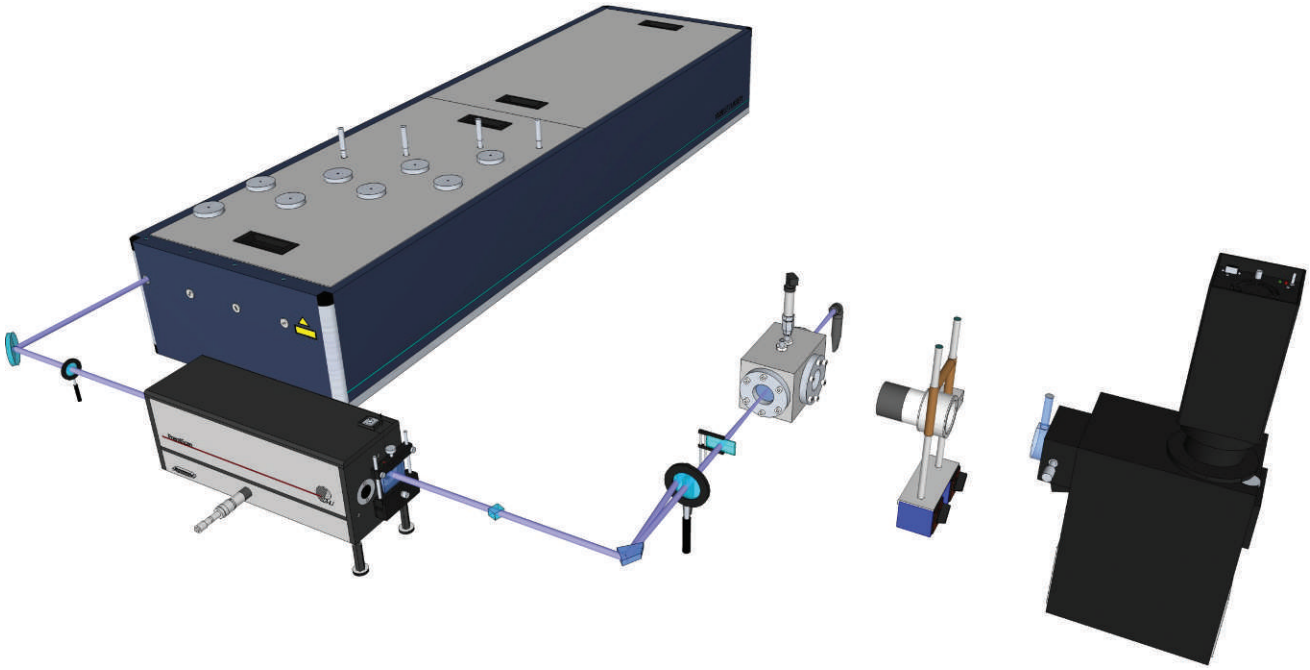

FIG. 2. Experimental setup. For the flame measurements a burner replaced the cell.

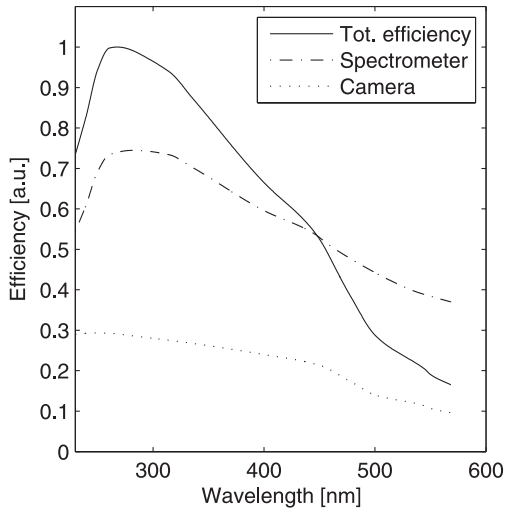

FIG. 3. Normalized total efficiency curve (solid) for the detection system and the efficiency curves for the spectrometer (dashed-dot) and the camera (dots), respectively.

10 mm and a tube length of 662 mm producing laminar, stable flow conditions for the premixed cone flame. Several different gas mixtures were investigated.

First, CO mixed with air, $\Phi = 2.0$, and a flow rate of 0.45 m/s was used. The measurements were performed at 9 mm in height above the burner (HAB). At this point the laser passed through the primary flame front, roughly a quarter of the way down from its tip.

Then premixed flames of methane and propane, with air as an oxidizer, were investigated. Measurements were done at three different equivalence ratios: $\Phi = 1.0$, 1.3, and 1.5. The flow rate of the gas mixture was 1 m/s except for the methane flame at $\Phi = 1.5$, where the flow rate was set to 0.6 m/s to shorten the flame cone. Two probing heights above the burner for the horizontal laser beam were selected, one slightly above the cone-shaped laminar primary flame-front and one positioned so that the laser passed through the primary flame front, at three-quarters of the first position's HAB. Fuel and air flows

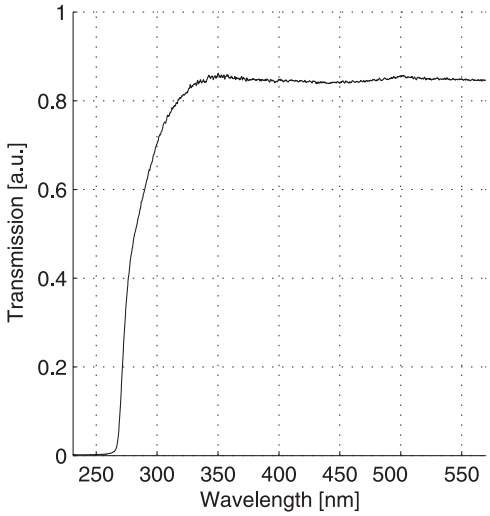

FIG. 4. Transmittance-curve of the N,N-dimethyl-formamide filter.

TABLE I. Methane and propane flame measurement matrix.

Φ	1.0	1.3	1.5
Methane			
Premixed flow rate	1 m/s	1 m/s	0.6 m/s
Flame front top (HAB)	13.5 mm	22.0 mm	25 mm
¾ of flame top (HAB)	10.1 mm	16.5 mm	18.5 mm
Propane			
Premixed flow rate	1 m/s	1 m/s	1 m/s
Flame front top (HAB)	13.6 mm	24.1 mm	–
¾ of flame top (HAB)	10.2 mm	18.0 mm	18 mm

were regulated by Bronkhorst mass-flow controllers. The entire measurement matrix can be seen in Table I.

RESULTS

Cell measurements. As mentioned previously, the pressure dependence of two-photon CO LIF was studied using a high-pressure cell. The resulting CO LIF emission spectra can be seen in Fig. 5. The spectra in the left column of Fig. 5 are recorded with 230 nm excitation and a pulse energy of 2.7 mJ, and the spectra in the right column are recorded with 217 nm excitation and a pulse energy of 1.3 mJ. The two emission spectra (Figs. 5A and 5B) were recorded with only 0.1 bar CO in the cell. Comparing Figs. 5A and 5B shows the difference in emission spectra from the two excitation schemes using 230 and 217 nm. It should be noted that some scattered light from the OPO fundamental can be seen in the right-hand spectra (Fig. 5B) as a distinct peak at 435 nm.

Notable is how the signal from the third positive system also appears in the spectra with 217 nm excitation (Fig. 5B). The peak intensities are, however, much lower than for 230 nm excitation due to lower transition probability caused by a larger energy gap between the $C^1\Sigma^+$ and the $b^3\Sigma^+$ states (see Fig. 1). The fact that they are detectable is very interesting as it suggests, in general, a rather large crossover from the singlet to the triplet states.

Also notable are the two small peaks at 440 and 470 nm in Fig. 5A. Comparing with modeled C_2 emission spectra (Fig. 6) these peaks are most likely from C_2. C_2 can be created by laser-induced photolysis of CO, as has been shown in previous studies.[15]

In Fig. 6 the mean integrated signal strength of the four strongest emission peaks in each emission band is shown as a function of the total pressure in the cell. The three curves represent the signal from the Ångström band with 230 nm excitation, the third positive band from the same measurements, and the Herzberg band after 217 nm excitation. For 217 nm excitation, the scattered laser fundamental coincides spectrally with the peak at 438 nm, as seen in Fig. 5B. Thus, this peak is not used in the evaluation, and the peak at 466 nm has been used instead.

All three curves show a decreasing signal level for increasing pressure. With increasing pressure the collisional time decreases, and hence the quenching time increase. The $C^1\Sigma^+$ state was expected to be less influenced by quenching due to its shorter lifetime.[6,23] However, the relative decrease in signal level is the lowest for the Ångström band, indicating that it is less sensitive to pressure compared to the other two bands. The $C^1\Sigma^{++}$ state has a larger transition rate to CO^+, and predissociation is also possible for lower rotational and vibrational numbers, which affect the quenching.[6] The signal

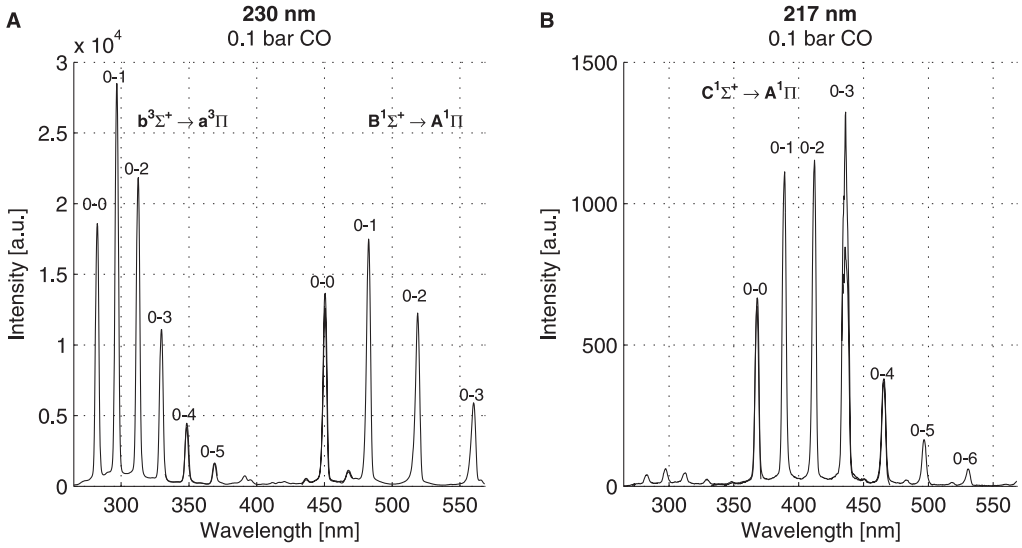

FIG. 5. CO LIF emission spectra acquired using the high pressure cell with 0.1 bar CO only. (**A, B**) Measurements with 230 nm, 2.7 mJ pulse energy (left), and 217 nm, 1.3 mJ pulse energy (right) excitation, respectively.

from the Herzberg band in this setup was a factor of 10 lower than the signal from the other two bands, due to lower laser pulse energies.

Figure 7 shows the CO LIF signals' pressure dependence when propane was added as a heavy quencher to the mixture in the cell.

Interestingly, the peaks from the third positive system decrease 90% when only 0.2 bar propane is added. The peaks in the Ångström and Herzberg bands decrease only ~50 %. This indicates that some molecules such as propane (C_3H_8) can affect the CO LIF signal from the third positive band significantly.

Modeled C_2-Crosstalk. Measurements of CO LIF were also performed in various flame environments to compare the applicability of the three excitation/detection schemes presented here in environments with spectral interferences from, e.g., C_2 and PAH.

Figure 8 shows two CO LIF emission spectra measured using the CO flame and a comparison with modeled CO emission spectra and modeled C_2 emission spectra. The efficiency of the camera and the spectrometer, seen in Fig. 3, has been compensated for.

For the modeled CO spectra, molecular constants and Franck Condon factors were taken from.[24] The modeled spectra further contain some assumptions to match them to the measured spectra from the CO flame. It was assumed that the vibration and rotation levels in the excited states were rapidly thermalized to a single temperature with an associated Boltzmann distribution. The temperature was chosen so that the relative peak intensity matched the measured spectra.

The transition probabilities between excited singlet states

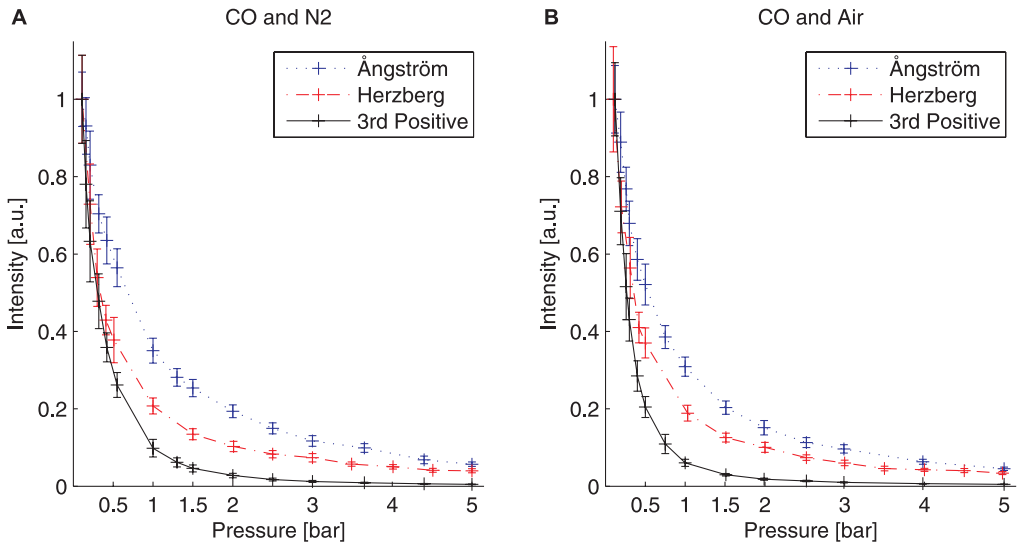

FIG. 6. CO LIF signal as a function of total pressure for increased N_2 (**A**) and air (**B**) partial pressure added to the initial 0.1 bar of CO. The curves represent 230 nm Ångström peaks (dashed), 217 nm Herzberg peaks (dash-dotted), and 230 nm third positive peaks (solid). The error bars indicate one standard deviation. The pulse energies were the same as in Fig. 5.

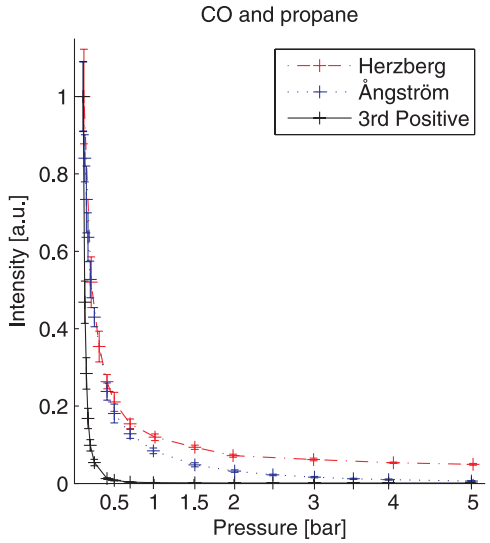

FIG. 7. CO LIF signal as a function of total pressure for increased propane partial pressure to the initial 0.1 bar CO. The curves represent: 230 nm Ångström peaks (dashed), 217 nm Herzberg peaks (dash-dotted), and 230 nm third positive peaks (solid). The error bars indicate one standard deviation.

and the triplet state were also modeled. The simplest assumption, that was adopted here, was to model the transitions with a constant probability for each electronic transition. The constants were selected so that the relative intensities between the bands matched the measured spectra from the CO flame.

An artificial line width was applied to the theoretical spectra. This was made by multiplying each transition line with a Gaussian function. The same line width was used for all peaks.

The C_2 spectrum was modeled assuming the same temperature distribution and artificial line width as used for the modeling of the 230 nm excitation CO spectra. Four electronic bands were found to have transitions in the spectral region of interest and were included in the model; the Swan band ($d^3\pi_g \rightarrow a^3\pi_u$), the Fox-Herzberg band ($e^3\pi_g \rightarrow a^3\pi_u$), the Mulliken band ($D^1\Sigma_u^+ \rightarrow X^1\Sigma_g^+$), and the Deslandres d'Azambuja band ($C^1\pi_g \rightarrow A^1\pi_u$).[25] The molecular constants for the electronic states, Frank Condon factors, and relative band strengths for C_2 were taken from the work of Cooper.[26]

The spectra in Fig. 8 clearly visualize the C_2 emission-spectral interferences with the CO LIF spectra. As expected the C_2 interference from the Swan band with the CO Ångström band reduces the number of available peaks for CO concentration measurements to just two, i.e., $v' = 0 \rightarrow v'' = 0$ and $v' = 0 \rightarrow v'' = 1$, confirmed in previous papers concerning CO LIF.[27] This usually reduces the signal-to-noise ratio of CO measurements in regions where C_2 is present or can be generated by the laser pulse, e.g., sooting or fuel-rich regions.

The Herzberg band also suffers from C_2 interference. In this case, the interference is not only from the Swan band, as for the CO Ångström band, but also from the Deslandres d'Azambuja band. Figure 8 indicates that the Herzberg system has two peaks that are without major C_2 interference and one (around 389 nm) that might suffer from some slight interference.

There appears to be less C_2 interference with the CO LIF peaks generated through the third positive system. The two strong peaks at 283 and 297 nm might have some interference from weak C_2 lines in the Fox-Herzberg band. However, as the upper state ($e^3\Pi_g$ around 5 eV) is highly energetic and quite close to the ionization energy of C_2, this band is expected to result in very low signal intensities. Between 300 and 340 nm there is no C_2 interference, and therefore at least three CO peaks in the third positive system should be available depending on the signal-to-noise ratio and the level of C_2 interference.

As both the Ångström and third positive bands are excited with the same laser wavelength of 230 nm, using the full spectra gives five peaks that do not suffer from any C_2 interference. This increases the signal to noise ratio significantly compared to measurements of solely the Ångström or Herzberg band.

Measured C_2-Crosstalk. Figure 9 shows LIF spectra recorded from the water-cooled laminar tube burner operating with premixed propane/air at $\Phi = 1.3$ and a flow rate of 1 m/s. The top row (Figs. 9A and 9B) shows measurements slightly above the primary reaction zone in the hot product gases. The bottom row (Figs. 9C and 9D) shows measurements through the primary flame front, at three-quarters the HAB of the measurements in Fig. 9A and 9B. Only the signal from the regions where the laser beam intersects the flame front is presented in Figs. 9C and 9D. The drop in signal level for wavelengths shorter than 270 nm is caused by the long-pass filter used to discriminate against scattered laser light; see Fig. 4.

As expected, some C_2 interferences can be seen in Figs. 9A and 9B, but it is very weak compared to Figs. 9C and 9D. In Figs. 9C and 9D, the C_2 emission peaks around 515 nm (III) and 470 nm (II) from the Swan band are clearly seen. It can be seen, quite clearly, when comparing Figs. 9A and 9C that only the 451 (f) and 484 nm (g) peaks of the Ångström band are free of interference from C_2.

Regarding the Herzberg band, in Fig. 9D, it can be seen that

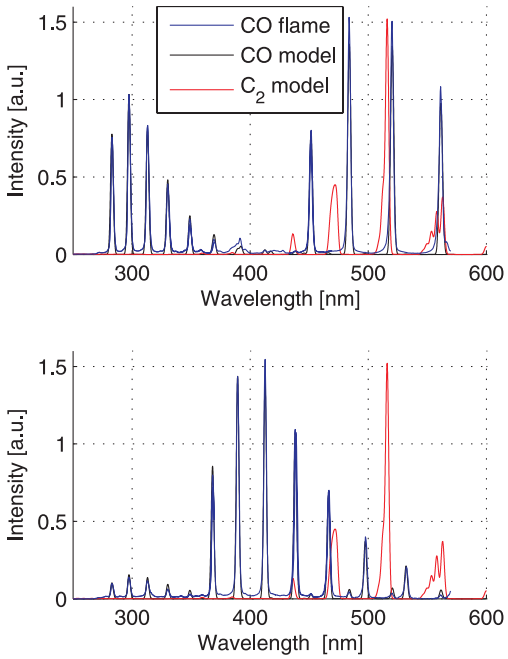

FIG. 8. CO LIF spectra taken in a CO flame (blue) for 230 nm excitation (top) and 217 nm excitation (bottom) compared to modeled CO emission spectra (black) and modeled C_2 emission spectra (red). Due to the good fit, the modeled CO emission spectra are hard to distinguish. We have taken account of the efficiency contributions of the camera and spectrometer.

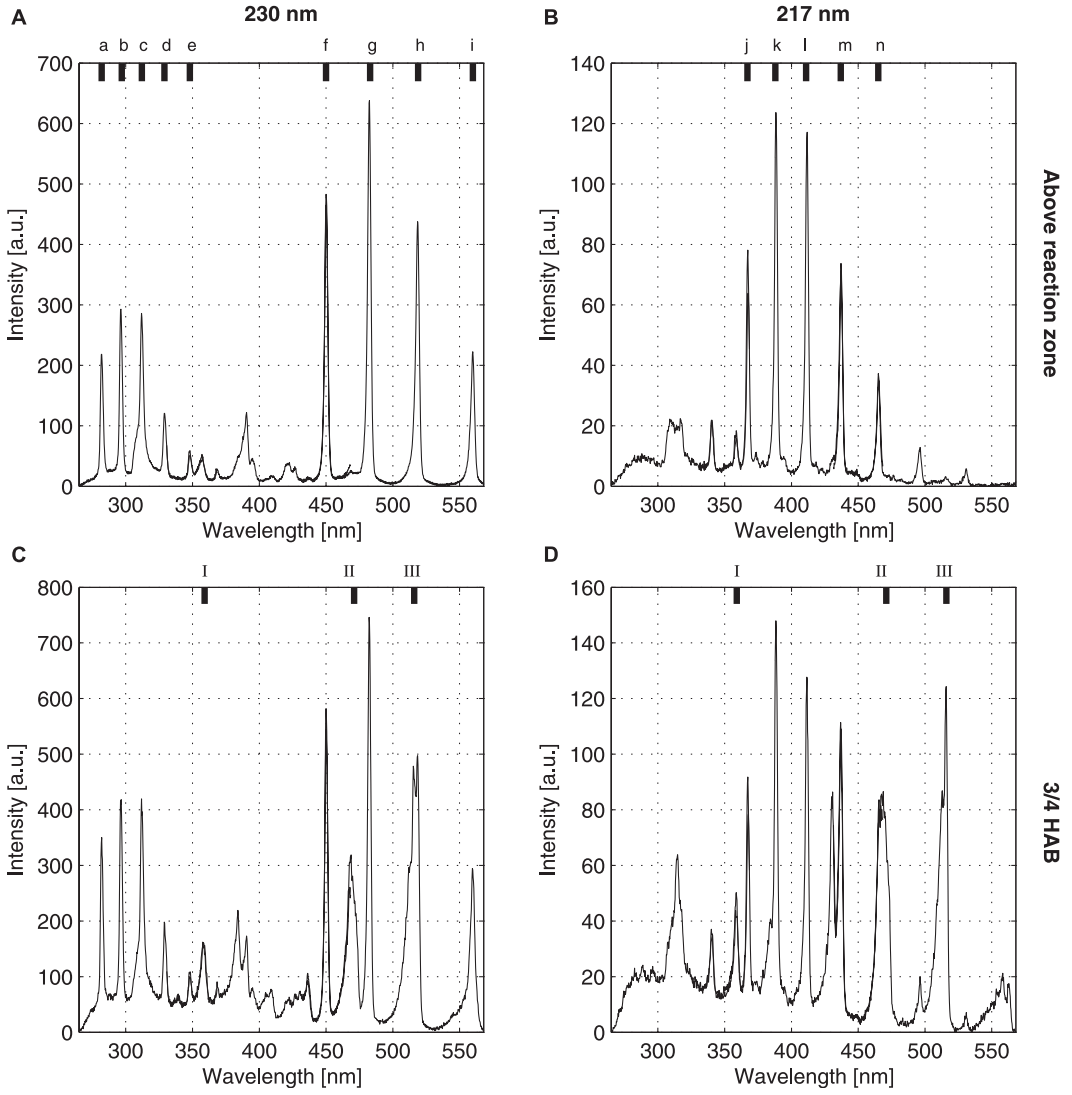

FIG. 9. CO LIF emission spectra recorded in a tube flame with premixed propane/air, $\Phi = 1.3$, and a flow rate of 1 m/s. The left and right columns show measurements with 230 and 217 nm excitation, respectively. The graphs in the top row (**A** and **B**) show spectra recorded with the laser beam slightly above the primary reaction zone. The bottom row graphs (**C** and **D**) show the spectra from the primary flame front, three-quarters of the HAB of the measurements in A and B. The lower case letters at the top of the graphs indicate the location of the CO peaks, and the roman letters show the location of the C_2 peaks.

the peak at 466 nm (n) is completely covered by C_2 emission. Also, the peak around 438 nm (m) is obviously severely disturbed by C_2 since the double-peak structure seen in Fig. 9D is not seen in Fig. 9B. A higher spectral resolution (up to a factor of 100 higher) will not separate these two lines according to modeled spectra with various line widths.

The peak around 389 nm (k) is widened at the base in Fig. 9D as compared to Fig. 9C. This is caused by the $\Delta v = 0$ transition in the Deslandres d'Azambuja ($C^1\pi_g \rightarrow A^1\pi_u$) C_2 band, which is situated spectrally close to this CO peak. Additionally, the peak at 360 nm (I) in Fig. 9D is caused by the $\Delta v = +1$ transition of the same C_2 band, indicating the possible level of C_2 interference in these measurements. This proves that even weaker bands such as the Deslandres d'Azambuja ($C^1\Pi_g \rightarrow A^1\Pi_u$) in the C_2 spectra can cause problems, and great care shall be taken when evaluating CO LIF spectra.

From the modeled C_2 spectra (Fig. 8) it can further be seen that the CO peak at 413 nm (l) overlaps with a week peak in the Deslandres d'Azambuja C_2 band (a factor 6 weaker than the peak at 385 nm). Thus, theoretically, only the CO peak around 368 nm (j) is completely without interference from C_2 LIF.

However, there is further broad-band interference with both the Herzberg and the third positive bands in the flame, probably from PAH LIF. As the interference is broadband it is easier to eliminate in the post processing compared to overlapping C_2 LIF signals.

Additionally the peaks from the third positive system do show some further interference. The peak at 313 nm (c) in Fig. 9C is clearly broadened due to overlap with another spectral structure. This peak is also seen in Figs. 9B and 9D. The remaining four peaks of the third positive band do not appear to have any C_2 interference. The overlap with the Fox-Herzberg C_2 band on the 283 nm (a) and 297 nm (b) peaks cannot be seen. Further, the relative strength between these peaks are consistent for both Figs. 9A and 9B, indicating no detectable C_2 interference.

Measurements were also conducted according to the test matrix in Table I with methane/air mixtures. These showed

similar trends as to Fig. 9 and the conclusions above. The methane flames gave slightly less C_2 and PAH interference in general.

CONCLUSION

This paper summarizes measurements of three different detection schemes for CO LIF measurements using two different excitation wavelengths. The spectral efficiency of the detection system was beneficial for detection of the third positive system, and consideration of this has also been reported.

Regarding C_2 interference, the detection scheme using the third positive band is comparable in quality to the Ångström band, or even slightly better. However, broadband emission from PAH clearly disturbs the third positive band. Nor is the Herzberg band free from disturbances due to C_2-crosstalk or broadband emission from PAH.

The third positive band shows stronger pressure and quenching dependencies compared to both the Ångström and the Herzberg band. A quantitative CO concentration measurement using the third positive band is thus harder, but not impossible.

The spectral interference from PAH and other species on the third positive band leads to the conclusion that qualitative imaging of CO using the third positive band is very hard to achieve. The best way (of the cases presented in this paper) to measure CO concentration is to spectrally resolve the full spectrum covering both the Ångström and third positive bands. This gives the maximum number of available CO LIF peaks and thus the best signal-to-noise ratio.

ACKNOWLEDGMENT

The authors gratefully acknowledge the financial support from CECOST and the ERC Advanced Grant "DALDECS."

1. M. Richter, Z.S. Li, M. Aldén. "Application of Two-Photon Laser-Induced Fluorescence for Single-Shot Visualization of Carbon Monoxide in a Spark Ignited Engine". Appl. Spectrosc. 2007. 61(1): 1-5.
2. K. Kohse-Höinghaus, J.B. Jeffries. Applied Combustion Diagnostics. New York: Taylor and Francis, 2002.
3. W.K. Bischel, B.E. Perry, D.R. Crosley. "Detection of Fluorescence from O and N Atoms Induced by Two-Photon Absorption". Appl. Opt. 1982. 21(8): 1419-1429.
4. M. Aldén, H. Edner, P. Grafström, S. Svanberg. "Two-Photon Excitation of Atomic Oxygen in a Flame". Opt. Commun. 1982. 42(4): 244-246.
5. R.P. Lucht, J.T. Salmon, G.B. King, D.W. Sweeney, N.M. Laurendeau. "Two-Photon-Excited Fluorescence Measurement of Hydrogen Atoms in Flames". Opt. Lett. 1983. 8(7): 365-367.
6. S. Linow, A. Dreizler, J. Janicka, E.P. Hassel. "Comparison of Two-Photon Excitation Schemes for CO Detection in Flames". Appl. Phys. B-Lasers O. 2000. 71(5): 689-696.
7. M.D. Di Rosa, R.L. Farrow. "Cross Sections of Photoionization and AC Stark Shift Measured from Doppler-Free B ← X(0, 0) Excitation Spectra of CO". J. Opt. Soc. Am. B. 1999. 16(5): 861-870.
8. M.D.D. Rosa, R.L. Farrow. "Temperature-Dependent Collisional Broadening and Shift of Q-Branch Transitions in the B←X(0,0) Band of CO Perturbed by N2, CO2 and CO". J. Quant. Spectrosc. RA. 2001. 68(4): 363-375.
9. T.B. Settersten, A. Dreizler, R.L. Farrow. "Temperature- and Species-Dependent Quenching of CO B Probed by Two-Photon Laser-Induced Fluorescence Using a Picosecond Laser". J. Chem. Phys. 2002. 117(7): 3173-3179.
10. F.D. Teodoro, J.E. Rehm, R.L. Farrow, P.H. Paul. "Collisional Quenching of CO B $^1\Sigma^+(v' = 0)$ Probed by Two-Photon Laser-Induced Fluorescence Using a Picosecond Laser". J. Chem. Phys. 2000. 113(8): 3046-3054.
11. M.D. Di Rosa, R.L. Farrow. "Two-Photon Excitation Cross Section of the B ← X(0,0) Band of CO Measured by Direct Absorption". J. Opt. Soc. Am. B. 1999. 16(11): 1988-1994.
12. S. Agrup, M. Aldén. "Measurement of the Collision-Quenched Lifetime of CO Molecules in a Flame at Atmospheric Pressure". Chem. Phys. Lett. 1992. 189(3): 211-216.
13. S. Agrup, M. Aldén. "Measurements of the Collisionally Quenched Lifetime of CO in Hydrocarbon Flames". Appl. Spectrosc. 1994. 48(9): 1118-1124.
14. B.J. Kirby, R.K. Hanson. "Planar Laser-Induced Fluorescence Imaging of Carbon Monoxide Using Vibrational (Infrared) Transitions". Appl. Phys. B: Lasers and Optics. 1999. 69(5–6): 505-507.
15. M. Aldén, S. Wallin, W. Wendt. "Applications of Two-Photon Absorption for Detection of CO in Combustion Gases". Appl. Phys. B-Lasers O. 1984. 33(4): 205-208.
16. J.M. Seitzman, J. Haumann, R.K. Hanson. "Quantitative Two-Photon LIF Imaging of Carbon Monoxide in Combustion Gases". Appl. Opt. 26. 1987. 26(14): 2892-2899.
17. P.J.H. Tjossem, K.C. Smyth. "Multiphoton Excitation Spectroscopy of the B $^1\Sigma^+$ and C $^1\Sigma^+$ Rydberg States of CO". J. Chem. Phys. 1989. 91(4): 2041-2048.
18. U. Westblom, S. Agrup, M. Aldén, H.M. Hertz, J.E.M. Goldsmith. "Properties of Laser-Induced Stimulated Emission for Diagnostic Purposes". Appl. Phys. B: Lasers and Optics. 1990. 50(6): 487-497.
19. D.A. Everest, C.R. Shaddix, K.C. Smyth. "Quantitative Two-Photon Laser-Induced Fluorescence Imaging of CO in Flickering CH4/air Diffusion Flames". Symposium (International) on Combustion. 1996. 26(1): 1161-1169.
20. J.E.M. Goldsmith, D.T.B. Kearsley. "C_2 Creation, Emission, and Laser-Induced Fluorescence in Flames and Cold Gases". Appl. Phys. B-Lasers O. 1990. 50(5): 371-379.
21. G. Anstett, G. Göritz, D. Kabs, R. Urschel, R. Wallenstein, A. Borsutzky. "Reduction of the Spectral Width and Beam Divergence of a BBO-OPO by Using Collinear Type-II Phase Matching and Back Reflection of the Pump Beam". Appl. Phys. B-Lasers O. 2001. 72(5): 583-589.
22. J. Sjöholm, E. Kristensson, M. Richter, M. Aldén, G. Göritz, K. Knebel. "Ultra-High-Speed Pumping of an Optical Parametric Oscillator (OPO) for High-Speed Laser-Induced Fluorescence Measurements". Sci. Technol. 2009. 20(2): 1-7.
23. T.A. Carlson, N. Duric, P. Erman, M. Larsson. "Correlation between Perturbation and Collisional Transfers in the A, B, C and b States of CO as Revealed by High Resolution Lifetime Measurements". Z. Phys. A-Hadrons Nucl. 1978. 287(2): 123-136.
24. P.H. Krupenie. The Band Spectrum of Carbon Monoxide. Washington, DC: U.S. Dept. of Commerce, National Bureau of Standards, 1966.
25. D.M. Cooper, R.W. Nicholls. "Measurements of the Electronic Transition Moments of C2-Band Systems". J. Quant. Spectrosc. RA. 1975. 15(2): 139-150.
26. D.M. Cooper. Absolute Measurements of the Electronic Transition Moments of Seven Band Systems of the C2 Molecule. [Ph.D. Thesis].Toronto: York University, 1979.
27. U. Aronsson, Ö. Andersson, R. Egnell, P.C. Miles, I.W. Ekoto. "Influence of Spray-Target and Squish Height on Sources of CO and UHC in a HSDI Diesel Engine during PPCI Low-Temperature Combustion". SAE Technical Paper. 2009. doi:10.4271/2009-01-2810.